The Journal of Chemical Physics

Dielectric spectra broadening as a signature for dipole–matrix interactions. V. Water in protein solutions

Cite as: J. Chem. Phys. **153**, 045102 (2020); https://doi.org/10.1063/5.0016437
Submitted: 04 June 2020 . Accepted: 05 July 2020 . Published Online: 23 July 2020

Larisa Latypova, Alexander Puzenko, Evgeniya Levy, and Yuri Feldman

The Journal of Chemical Physics ARTICLE scitation.org/journal/jcp

Dielectric spectra broadening as a signature for dipole–matrix interactions. V. Water in protein solutions

Cite as: J. Chem. Phys. 153, 045102 (2020); doi: 10.1063/5.0016437
Submitted: 4 June 2020 • Accepted: 5 July 2020 •
Published Online: 23 July 2020

Larisa Latypova,[1,2] Alexander Puzenko,[1] Evgeniya Levy,[1] and Yuri Feldman[1,a)]

AFFILIATIONS

[1] Department of Applied Physics, The Hebrew University of Jerusalem, Givat Ram, Jerusalem 91904, Israel
[2] Department of Physics, Kazan Federal University, 18 Kremlewskaya St., 420008 Kazan, Russia

[a)] Author to whom correspondence should be addressed: yurif@mail.huji.ac.il

ABSTRACT

In this paper, the fifth of our series focused on the dielectric spectrum symmetrical broadening of water, we consider the solutions of methemoglobin (MetHb) in pure water and in phosphate-buffered saline (PBS). The universal character of the Cole–Cole dielectric response, which reflects the interaction of water dipoles with solute molecules, was described in Paper I [E. Levy *et al.*, J. Chem. Phys. **136**, 114502 (2012)]. It enables the interpretation of the dielectric data of MetHb solutions in a unified manner using the previously developed 3D trajectory method driven by the protein concentration. It was shown that protein hydration is determined by the interaction of water dipoles with the charges and dipoles located on the rough surfaces of the protein macromolecules. In the case of the buffered solution, the transition from a dipole-charged to a dipole–dipole interaction with the protein concentration is observed {see Paper III [A. Puzenko *et al.*, J. Chem. Phys. **137**, 194502 (2012)]}. A new approach is proposed for evaluating the amount of hydration water molecules bounded to the macromolecule that takes into account the number of positive and negative charges on the protein's surface. In the case of the MetHb solution in PBS, the hydration of the solvent ions and their interaction with charges on the protein's surface are also taken into consideration. The difference in hydration between the two solutions of MetHb is discussed.

I. INTRODUCTION

It has become increasingly clear over the past two decades that water is not simply "life's solvent." Instead, water forms an active matrix that engages and interacts with all the molecules dissolved in it. This interaction is complex, subtle, and essential.[1,2] While the extraordinary physical and chemical properties of liquid water have long been acknowledged, the majority of biologists still underestimate the active role of water and consider it a passive environment, in which life's molecular components are arrayed. Recent evidence contradicts this view. The hydration shell of any molecule, be it inorganic salt, lipid, sugar, or protein, manipulates the molecule's "active volume," effectively changing its charge, size, and structure.[3–6] Remarkably, the structure and dynamics of this shell feed back into the distinct functional properties of the cellular solutes and macromolecules.[7] Therefore, the experimental characterization and quantification of the state of water and its properties in complex biological systems remains one of the most momentous challenges of our century. Specifically, the significant question remains as to how to link the dynamic properties of the water around biomolecules with the surrounding hydrogen-bonding network of bulk water. It is clear that the H-bond network, its fluctuations, and the dynamics of its rearrangement determine the properties of solvated biomolecules.[8] The hydration shell and its influence on the protein have been studied extensively over the last few decades using a variety of experimental techniques.[9–13] Due to water's high polarity, dielectric spectroscopy (DS) is a particularly suitable method for studying water structure and dynamics in complex materials. It is well known that over a wide temperature range and at frequencies up to 40 GHz, the complex permittivity spectra of the bulk water (see Fig. 1, black line[5]) can be described well by the simple Debye function,[14,15] which corresponds to the single exponential decay function of the polarization. However, whenever water interacts with another dipolar or charged entity, a symmetrical broadening of its dielectric

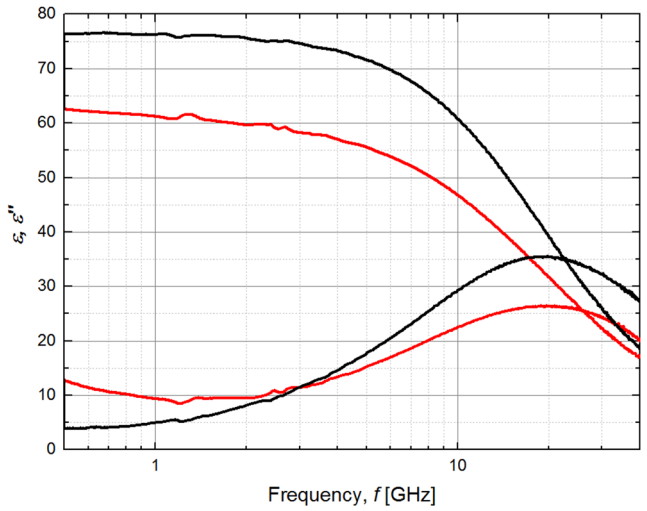

FIG. 1. Real $\varepsilon'(f)$ and imaginary $\varepsilon''(f)$ parts of the complex permittivity of bulk water (black curves) and aqueous solution of methemoglobin (MetHb) solutions (30 mg/dl) (red curves) at 25 °C.

loss peak occurs (see Fig. 1, red line).[16,17] The origin of the main dispersion peak broadening is defined by the dynamics of H-bond network rearrangements in the vicinity of different solute molecules. One can clarify the nature of the interaction of the hydration shell of the solute, be it dipole–dipole or charge–dipole, by studying how the concentration of the solute influences the broadening. Note that in aqueous solutions, the dielectric response of the hydration water shell is negligible and thus cannot be directly detected in dielectric experiments, despite numerous attempts in recent decades.[18–22] The broadening of the main water relaxation peak in aqueous solutions can be described by the phenomenological Cole–Cole (CC) function,[23]

$$\varepsilon^*(\omega) = \varepsilon'(\omega) - i\varepsilon''(\omega) = \varepsilon_h + \frac{\Delta\varepsilon}{1 + (i\omega\tau)^{\alpha}}. \quad (1)$$

Here, ε' and ε'' are the real and imaginary parts of the complex permittivity, $\omega = 2\pi f$ is the cyclic frequency, and $i^2 = -1$. The parameter ε_h denotes the ultimate high-frequency permittivity (an adjustable parameter, which was fixed at 4.5 as described in Paper II[4]), and $\Delta\varepsilon = \varepsilon_l - \varepsilon_h$ is the relaxation amplitude (with the low frequency permittivity limit denoted by ε_l). The parameter τ is the relaxation time. The exponent α ($0 < \alpha \leq 1$) is a measure of the symmetrical broadening. In the case of pure water, for frequencies up to 40 GHz, α can be set to 1, resulting in a Debye relaxation.[24]

The main feature of dielectric properties of any aqueous solution is the decrement of dielectric permittivity compared to bulk water (Fig. 1). Another typical peculiarity is the symmetrical spectra broadening with changes in relaxation time. Here, water is considered the dipole subsystem, and the solute molecules play the role of the matrix. As shown in Papers II–IV,[3–6] water dipole–matrix interactions lead to a CC broadening of the spectrum and its shift in frequency, depending on the type of interactions. The direction of the frequency shift is ascertained by the matrix's type (ionic or dipole). If a solute has a dipole nature, the dipole–dipole interactions lead to an increase in relaxation time τ with an increase in the solute concentration—the so-called "red shift" of the frequency of the maximum of water dispersion.[3,6] In the case of electrolytes, the so-called "blue shift" is observed due to dipole–ion interactions. The well-known decrease of the experimental relaxation time in electrolyte solutions can be attributed to a shrinking of mesoscopic water clusters.[4,25] If a solute molecule has both charged and dipole groups, the measured response is affected by the predominance of the dipole–dipole or dipole–ion interactions, depending on their relative concentration.[5]

We presented a number of works, where the most general cases of dipole–matrix interactions were considered.[16,17,26,27] However, a knowledge gap still exists in the understanding of water behavior in protein solutions. Proteins are made up of long chains of amino acids. There are 20 different types of amino acid, each of which has a unique side radical.[28] The linear sequence of amino acids within a protein is considered the primary structure of the protein. The primary structure of a protein drives the folding and intramolecular bonding of the linear amino acid chain, which ultimately determines the protein's unique three-dimensional shape. Known as α-helices and β-sheets, these stable folding patterns make up the secondary structure of a protein.[28] Most proteins contain multiple helices and sheets, in addition to other less common patterns. The ensemble of formations and folds in a single linear chain of amino acids—sometimes called a polypeptide—constitutes the tertiary structure of a protein.[28] Finally, the quaternary structure of a protein refers to those macromolecules with multiple polypeptide chains or subunits.[28]

Dipole and charged groups are distributed on the surface of the macromolecule and in the aqueous environment. Therefore, competition takes place between dipole–ion and dipole–dipole interactions in such a system. Following the approach based on the fractal nature of the time set of the relaxing water dipoles' interaction with their encompassing matrix,[16] it is natural to contemplate a physical concept underlying the CC broadening in aqueous protein solutions. The approach is based on 3D trajectories constructed from all of the parameters of the CC spectra [Eq. (1)] and has been used to describe the state of water interacting in non-ionic,[3] ionic,[4] and nucleotide[5] solutions. This method demonstrates a fundamental connection between the relaxation time τ, the broadening parameter α, and the Kirkwood–Froehlich correlation function B, which is the function on $\Delta\varepsilon$.[16] The parameters B, τ, and α were chosen as the basis for the coordinates of a new 3D space, wherein the evolution of the relaxation process, as a result of the variation of an external macroscopic parameter (temperature, concentration, pressure, etc.), will depict a trajectory. This trajectory is a result of the connection between the kinetic and structural properties of water in the hydration environment. The 3D trajectory approach is applied in this article to calculate the dynamic and structural characteristics of the methemoglobin (MetHb) solution at different concentrations. MetHb is one of the most investigated proteins to date.[29] It is known that biological macromolecules perform their function in specific cellular environments (subcellular compartments or tissues); therefore, they are adapted to the biophysical characteristics of the corresponding environment, one of them being the characteristic pH.[30] In order to maintain an environment similar to

that of physiological conditions, the dielectric measurements were carried out in phosphate-buffered saline (PBS) with pH = 7.4. As the control, the MetHb solution at different concentrations was measured in double-distilled water (DDW).

II. MATERIALS AND METHODS

A. Sample preparation

Lyophilized powder of human hemoglobin was obtained from Sigma Aldrich (H7379). Solutions of MetHb (30 g/dl, 25 g/dl, 20 g/dl, 15 g/dl, 10 g/dl, 7 g/dl, and 5 g/dl) were prepared in double-distilled water (DDW) and in phosphate-buffered saline (PBS) with pH = 7.4 at 25 °C.

B. Microwave dielectric spectroscopy

Dielectric measurements were carried out in the frequency range from 500 MHz to 40 GHz using a microwave vector network analyzer (Keysight N5234B PNA-L) together with a flexible cable and slim-form probe (Keysight N1501A Dielectric Probe Kit). System calibration was performed using three references: air, a Keysight standard short circuit, and pure water at 25 °C. Calibration was supported using the E_{cal} mode. A special stand for the slim-form probe was designed and combined with a sample cell holder for liquids (total volume ~ 7.8 ml). The holder was temperature-regulated via a thermostat connected to a Julabo CF 41 oil-based heat circulatory system. The temperature was maintained at 25 ± 0.1 °C. Each curve corresponding to MetHb in DDW and in PBS was measured at least six times, where each measurement took ~30 s. The real and imaginary parts $\varepsilon'(\omega)$ and $\varepsilon''(\omega)$ were evaluated using the Keysight N1500A Materials Measurement software with an accuracy of $\Delta\varepsilon'/\varepsilon' = 0.05$ and $\Delta\varepsilon''/\varepsilon'' = 0.05$.

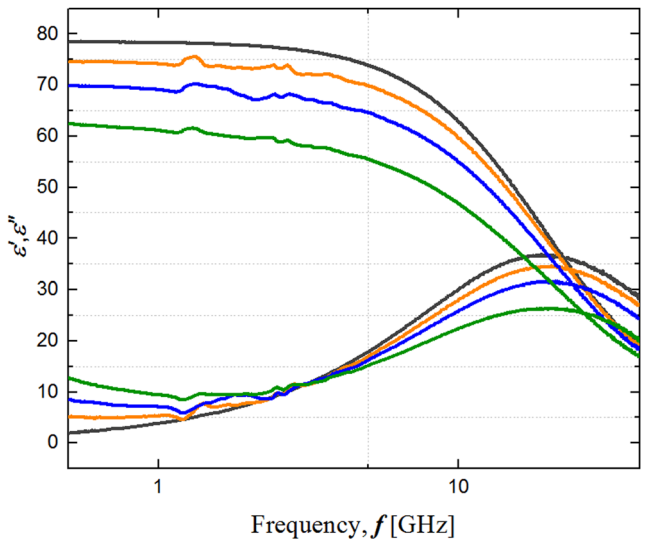

FIG. 2. The real part $\varepsilon'(f)$ and the imaginary part $\varepsilon''(f)$ of the dielectric spectra of DDW (black line) and aqueous solutions of MetHb at concentrations of 7 g/dl (orange line), 15 g/dl (blue line), and 30 g/dl (green line) at 25 °C.

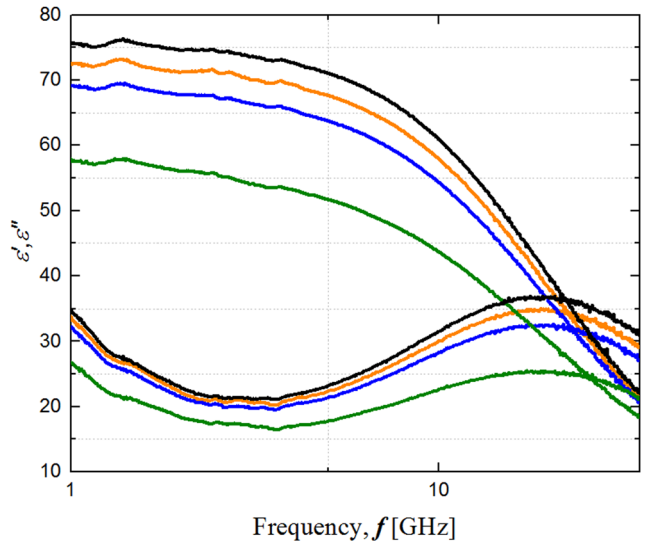

FIG. 3. The real part $\varepsilon'(f)$ and the imaginary part $\varepsilon''(f)$ of the dielectric spectra of PBS (black line) and aqueous solutions of MetHb at concentrations of 5 g/dl (orange line), 15 g/dl (blue line), and 30 g/dl (green line) at 25 °C.

III. RESULTS AND DATA PROCESSING

Typical dielectric spectra of aqueous solutions of MetHb in both PBS and DDW at various concentrations are presented in Figs. 2 and 3, respectively.

The spectra were fitted with Eq. (1) (CC relationship) using an in-house fitting software Datama.[31] During the fitting procedure, ε_∞ was fixed at 4.5, corresponding to a recent procedure employed by Buchner *et al.*[32] Fitting parameters (relaxation time τ, broadening parameter α, and dielectric strength $\Delta\varepsilon$) for solutions of MetHb both in DDW and PBS saline are presented in Table II (Appendix A).

IV. DISCUSSION

Following the protocol of Papers I–IV of the series[3–6] and using the CC parameters obtained from the fitting routine, the 3D trajectories for solutions of MetHb in DDW and PBS are considered. The specific 3D space is defined by the rectangular coordinates $X = \ln B$, $Y = \ln \tau$, and $Z = \alpha$, where B is Froehlich's function[16,33] at temperature T,

$$B = \Delta\varepsilon(\mathrm{T})\frac{2\varepsilon_l(T) + \varepsilon_h}{3\varepsilon_l(T)}. \tag{2}$$

The 3D trajectories, as well as their projections, are quite different for both solutions. A detailed analysis of the different dependences of α upon the variable $x = \ln \tau$ shows that all of them can be summarized by one universal function [Eq. (3)],

$$\alpha = A + \frac{G}{x - x_0}. \tag{3}$$

This equation demonstrates a hyperbolic curve bounded by two asymptotes: the constant A, representing the asymptotic value of the parameter α, and the asymptote $x_0 = \ln \tau_c$, dividing the full plane into two semi-planes: $\tau > \tau_c$ and $\tau < \tau_c$ (Fig. 4). It was shown that the

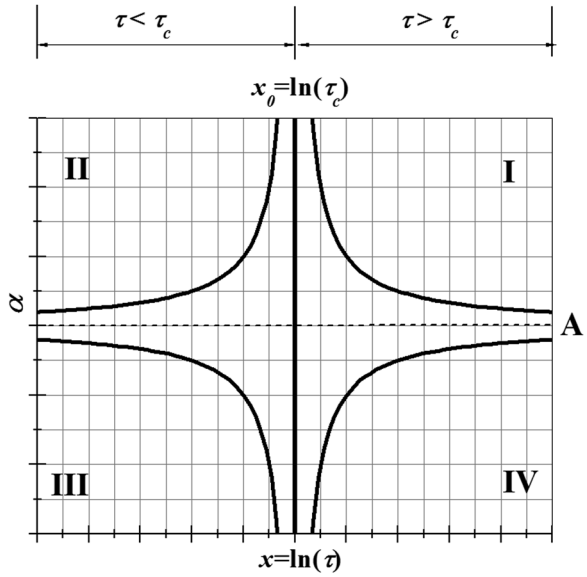

FIG. 4. The four hyperbolic branches of the function defined by Eq. (3). Reprinted with permission from A. Puzenko, P. Ben Ishai, and Yu. Feldman, Phys. Rev. Lett. **105**, 037601 (2010). Copyright 2010 AIP Publishing LLC.

first quadrant of the plane ($\tau > \tau_c$, $\alpha > A$) determines a dipole–dipole interaction between the matrix and the bulk.[3] The second quadrant of the plane ($\tau < \tau_c$, $\alpha > A$) determines a dipole–ion interaction (Fig. 4).

Applying the fitting function (3) to the experimental pattern $\alpha(\ln\tau)$ and substituting the fitting parameters A, G, and x_0 into model equations [Eqs. (2) and (4)], we obtain

$$N_{0\tau} = \exp(G), \quad \tau_c = \exp(x_0), \quad N_\tau = N_{0\tau}\left(\frac{\tau}{\tau_c}\right)^A. \tag{4}$$

We can calculate the following parameters: cutoff relaxation time τ_c; the number of elementary relaxation events during this time $N_{0\tau}$, and N_τ the number of relaxation events τ during the experimental relaxation time τ. The 3D trajectories for the MetHb solution in DDW and PBS using the described routine are plotted in Fig. 5.

It is clear that the 3D trajectories depict the specificity of the protein structure and the type of interaction with the solvent. However, the understanding of the kinetics, structure, and hydration process in solutions can be expanded by considering various 2D projections. While for the MetHb solution in DDW, the $\alpha(\ln\tau)$ dependence corresponds to the first quadrant [see Figs. 5(a) and 6(a)], the same projection $\alpha(\ln\tau)$ for MetHb in PBS demonstrates the transition from the second quadrant ($\tau < \tau_c$; $\alpha > A$) to the first ($\tau > \tau_c$; $\alpha > A$) [see Figs. 5(b) and 6(b)]. It is clear from Figs. 5(b) and 6(b) that at high concentrations, the function $\alpha(\ln\tau)$ moves to the first quadrant, similar to what occurs in monosaccharide solutions.[3] Thus, at high Hb concentrations, the dipole–dipole interactions are dominant, while at low concentrations, the dipole–ion interactions between water and the PBS buffer ions prevail over the water–Hb interactions, and the corresponding curve appears in the second quadrant [see Fig. 6(b)]. Furthermore, both MetHb solutions are characterized by different cutoff times τ_c that correspond to different branches of Eq. (3). All values of τ_c and $N_{0\tau}$ were calculated using Eqs. (3) and (4). The values of τ_c and $N_{0\tau}$ for MetHb in PBS and DDW are presented in Table I.

In the low concentration region ($\tau < \tau_c$, second quadrant) for MetHb in PBS, the asymptotic value τ_c approaches the values typical to those of the ionic solutions: $\tau_c = 8.24$ ps and $N_{0\tau} \cong 1$. At the

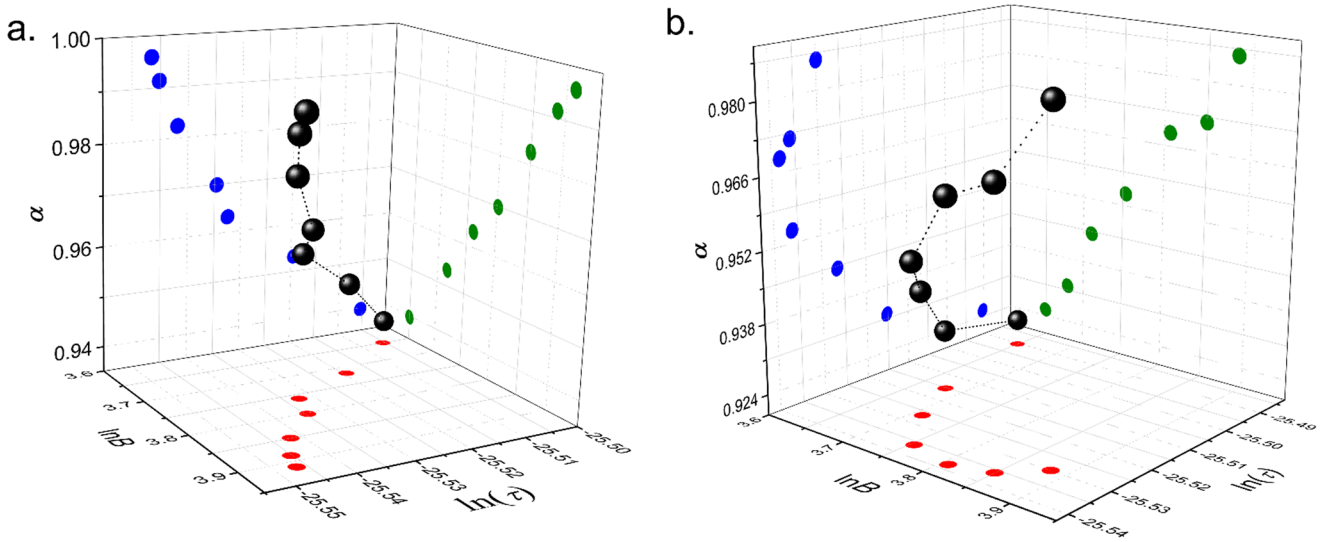

FIG. 5. 3D trajectories of the CC relaxation process for MetHb solution in DDW (a) and MetHb in PBS (b) at 25 °C.

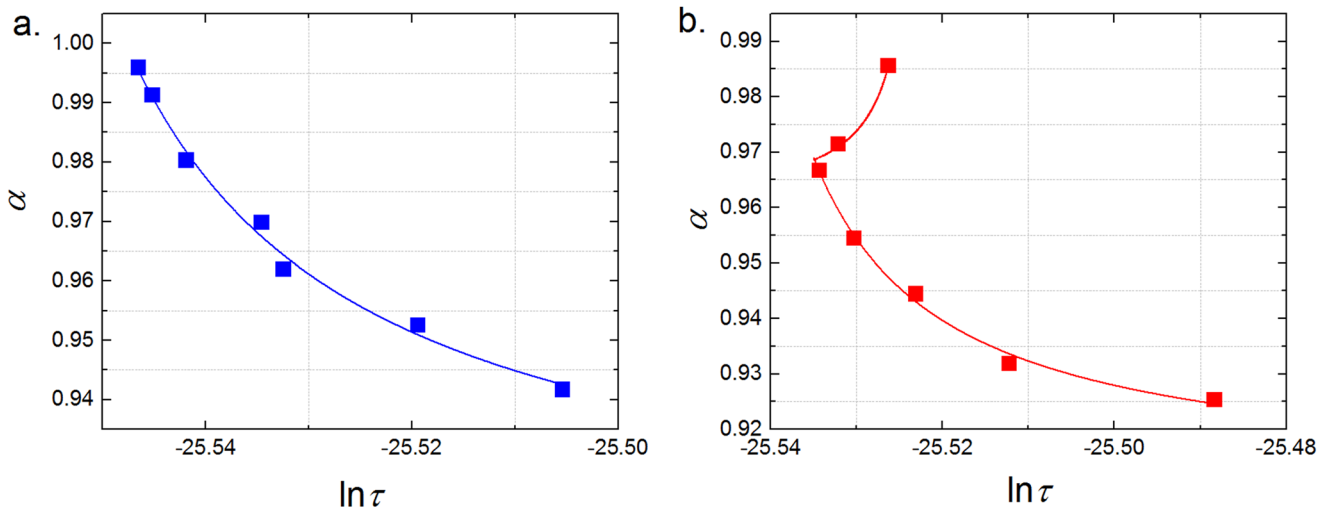

FIG. 6. The $\alpha(\ln \tau)$ dependences for the solution of MetHb in DDW (a) and MetHb in PBS (b) at 25 °C [solid lines show the fitting results using Eq. (4)].

same time, for MetHb in DDW, $\alpha(\ln \tau)$ dependence is in the first quadrant for all protein concentrations, $\tau_c \cong 7.85$ ps and $N_{0\tau} \cong 1$. In both cases, the asymptotic values of τ_c in the first quadrant are significantly higher than in the case of simple nonionic solutions[3] but slightly smaller than in the case of the relaxation of bulk water.

We recently put forward[25] that the experimental relaxation time of bulk water is associated with a minimal size of water clusters. This suggests that water clusters in both MetHb solutions (in PBS and DDW) are smaller than those of the bulk water. Furthermore, the value $N_{0\tau} \cong 1$ for both solutions indicates a single relaxation associated with water clusters of smaller size compared to the bulk water.

In order to evaluate the structure of the solution from 3D trajectories, Froelich's function [Eq. (2)] can be presented in terms of the total fluctuating dipole moment $\boldsymbol{M}$ of the system,[33]

$$B = \frac{1}{3\varepsilon_0 k_B T} \cdot \frac{\langle \boldsymbol{M} \rangle^2}{V}. \tag{5}$$

Here, T is the absolute temperature, ε_0 is the dielectric permittivity of the vacuum, k_B is Boltzmann's constant, and V is the volume of the sample. For the solution of MetHb in DDW, the random implementation of the system's dipole moment vector can be presented as follows:

$$\boldsymbol{M}_{DDW} = \sum_{i=1}^{N_{free}} \boldsymbol{\mu}_i + \boldsymbol{M}_{HB}, \tag{6}$$

where $\boldsymbol{\mu}_i$ is the dipole moment of a water molecule, and $\boldsymbol{M}_{HB}$ is the dipole moment of the Hb macromolecule surrounded by bound water. The number of free water molecules in the sample—N_{free}—is defined as the difference between their number in bulk and the number of water molecules associated with MetHb molecules at a given concentration. The function B, defined by Eqs. (2) and (5), establishes the relationship between the experimental values of the dielectric strength for the main water process in the Hb solution and the mean square $\langle \boldsymbol{M}^2 \rangle$ of the fluctuation dipole moment (6). In order to calculate $\langle \boldsymbol{M}^2 \rangle$, we assumed the following:

a. The interaction between the free water dipoles is described by the Kirkwood correlation factor; [25,33]
b. Due to the hydrophobic effect, the bound water molecules in the hydration shells of various charges of the same sign do not interact with one another;
c. The interactions of free and bound water in the shells of charged groups can be neglected. This interaction is reduced to the exchange between free water molecules and water molecules in the external hydrating layer.

TABLE I. Values of τ_c and $N_{0\tau}$ for MetHb in DDW and MetHb in PBS.

	$N_{0\tau}$		τ_c (ps)	
	1		7.85	
	The low concentration branch: $\tau > \tau_c, \alpha > A$		The high concentration branch: $\tau < \tau_c, \alpha > A$	
MetHb in DDW	$N_{0\tau}$	τ_c (ps)	$N_{0\tau}$	τ_c (ps)
MetHb in PBS	1	8.24	1	8.03

Obviously, the contribution of this surface effect to the dielectric response is small compared to the contribution of bulk water. Substituting (B7) (see Appendix B) into Eq. (5) and equating the right-hand sides of relations (2) and (5), we can determine the volume concentration of hydrated water molecules $n_b^{(DDW)}$ associated with the *Hb* globules. For MetHb solution in DDW, we obtain

$$n_b^{(DDW)} = n_0 \frac{1 - \frac{B_{exp}}{B_{exp}^{(0)}}}{\left(1 + \frac{4}{g_w}\left(\frac{n_p}{n_p+n_n}\right)^2\right)}. \tag{7}$$

Here, $n_0 = \frac{N_0}{V}$ is the volume concentration of the bulk water molecules (N_0 is the number of bulk water molecules in volume V), and $n_p = \frac{N_{Hb}N_p}{V}$ and $n_n = \frac{N_{Hb}N_n}{V}$ are the concentrations of positive and negative charges assigned to MetHb macromolecules, respectively. In (7), $B_{exp}^{(0)}$ and B_{exp} are the experimental functions for the bulk water and for the particular molar concentration of MetHb, respectively; g_w is the Kirkwood factor for the bulk water,[24,32] and n_p and n_n are the concentrations of the positive and negative charges on the surface of MetHb macromolecules, respectively.

However, in the case of MetHb in the buffer solution, we must take into account the number of water molecules associated with ions (Na^+, Cl^-, K^+, HPO_4^{2-}, and $H_2PO_4^-$) of PBS. To do this, we must introduce an additional term $\Delta\boldsymbol{M}$ to $\boldsymbol{M}_{DDW}$ in Eq. (6),

$$\boldsymbol{M}_{PBS} = \boldsymbol{M}_{DDW} + \Delta\boldsymbol{M}, \tag{8}$$

which can be presented as

$$\Delta\boldsymbol{M} = \sum_{i=1}^{N_{jp}} \sum_{k=1}^{N_{jw}^+} \boldsymbol{\mu}_{ik} + \sum_{i=1}^{N_{jn}} \sum_{k=1}^{N_{jw}^-} \boldsymbol{\mu}_{ik}. \tag{9}$$

Here, the summation index i is related to the number of ions in the buffer with the upper limits of their total positive and negative numbers N_{jp} and N_{jn} in the volume V, respectively (the index j is assigned to the buffer ions). The second summation index k is related to the number of water molecules bounded by all positive and negative ions with the upper limits N_{jw}^+ and N_{jw}^-, respectively. For the approximate calculation of the mean square of the fluctuation dipole moment $\langle \boldsymbol{M}_{PBS}^2 \rangle$ of MetHb in the PBS solution, the following additional assumptions are required:

(a) The interaction between the shells around PBS ions with the same sign is negligible;
(b) Due to the mixture of different PBS ions that include both phosphates and simple salts, we must assume that $N_{jp} > N_{jn}$. Therefore, we can consider the number of PBS buffer ions as the sum of N_{jn} coupled ions and the rest, $\Delta N_{jp} = N_{jp} - N_{jn}$ of positive ions. Taking into account that on the surface of the MetHb macromolecule, there are more negative charges than positive ($N_n > N_p$), we can assume that the rest of the negative charges $\Delta N_n = N_n - N_p$ of MetHb are compensated by the rest of the positive ions ΔN_{jp} of PBS.

Under these assumptions, we can calculate $\langle \boldsymbol{M}_{PBS}^2 \rangle$ for the MetHb solution in PBS (see Appendix C). Using the same routine as for MetHb in DDW, we can determine the concentration of water molecules n_b associated with the MetHb macromolecules in the buffer as follows:

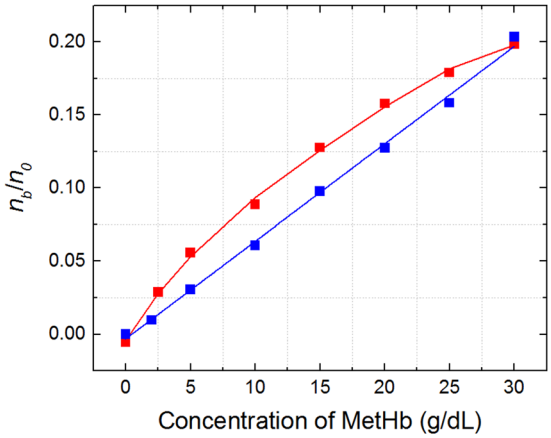

FIG. 7. Volume concentrations $\boldsymbol{n_b^{(DDW)}}$ of water molecules bounded by MetHb in DDW solution and concentration $\boldsymbol{n_b^{(PBS)}}$ of water molecules bound by MetHb in PBS solution normalized to the volume concentration $\boldsymbol{n_0}$ of water molecules in the pure bulk water.

$$n_b^{(PBS)} = n_0 \frac{1 - \frac{B_{PBS}}{B_{PBS}^{(0)}} - \frac{n_{jwb}}{n_0}\left[1 - \frac{1}{g_w} + \frac{4}{g_w}\left(\frac{n_{jn}}{n_{jn}+n_{jp}}\right)^2\right]}{\left[1 + \frac{4}{g_w}\left(\frac{n_p}{n_p+n_n}\right)^2 + \frac{4}{g_w}\left(\frac{n_{jp}}{n_{Hb}\Delta N_n+n_{jp}}\right)^2\right]}, \tag{10}$$

where n_{jwb} is the concentration of water molecules in the hydration shells of solvent ions, n_{jn} and n_{jp} are the concentrations of the negative and positive ions of PBS, respectively, and n_{Hb} is the concentration of MetHb (see Appendix C).

The ratios of the volume concentrations of water molecules $n_b^{(DDW)}$ and $n_b^{(PBS)}$ bounded by MetHb in DDW and PBS solutions, respectively, to the volume concentration of the bulk water molecules are calculated using Eqs. (7) and (10) and are presented in Fig. 7 as a function of the MetHb concentration. It is clear that the number of hydrated molecules in the MetHb PBS solution is higher than in DDW. Furthermore, the influence of the additional dipole contribution due to the PBS coupled ions considerably modifies the concentration dependence of hydrated water and makes it nonlinear. The transition to nonlinear behavior in PBS occurs at the same MetHb concentration, at which the projection $\alpha(\ln\tau)$ from the 3D trajectory shifted from the second to the first quadrant [see Figs. 5(b) and 6(b)]. It also corresponds to the extremum observed in the projection $\ln B(\ln\tau)$ for the 3D trajectory [see Fig. 5(b)].

V. CONCLUSIONS

With this work, we complete the cycle of studies concerning the dielectric relaxation of water in aqueous solutions in a number of biological objects: monosaccharides, ions, nucleotides, amino acids, and proteins. Despite the universal nature of the CC dielectric response, which reflects the interaction of water dipoles with solute molecules, their hydration is quite different. In the simplest case of ionic solutions, the hydration is determined by the dipole–charge interaction. In the case of amino acids and nucleotides, the hydration is determined either by the dipole–dipole interaction or

by a mixed type of interaction with a transition from a dipole–ion to a dipole–dipole type. In the case of proteins, the size of the macromolecules is significantly larger than the size of the water dipole. The hydrophilic interaction of water molecules with charges and dipoles localized on the surface of proteins occurs on the rough surface of the macromolecule. In the case of a solution of MetHb in PBS, the hydration of the solvent ions and their interaction with charges on the surface of the protein are taken into account. These results have made it possible to unravel the mechanisms governing the role of water in protein hydration.

AUTHORS' CONTRIBUTIONS

All authors contributed equally to this work.

ACKNOWLEDGEMENTS

The authors would like to thank Keysight Technologies Israel Ltd. and INTERLLIGENT RF and Microwave Solutions for the loan of the Vector Network Analyzer Agilent N5234B PNA-L. They would like to thank the Swiss National Science Foundation, Grant No. CRSII5_180234, for their financial support for the Research Project "Premembrane and cytosolic water as a marker of red blood cell aging *in vivo* and *in vitro*." They would also like to thank ISF Grant No. 341/18 for the financial support for this research project.

There are no conflicts to declare.

APPENDIX A: DIELECTRIC PARAMETERS FOR MetHb SOLUTIONS IN DDW AND PBS AT VARIOUS CONCENTRATIONS AT 25 °C

TABLE II. Parameters of the Cole–Cole relaxation spectral function [Eq. (1)] for MetHb solutions in DDW and PBS at various concentrations at 25 °C (ε_∞ has been fixed at 4.5).

	$\Delta\varepsilon$	τ (ps)	α	σ (S/m)
C (g/dL)	±1%	±2%	±0.5%	±1%
Dielectric parameters of the MetHb solution in DDW at 25 °C				
2	72.94	8.04	0.996	0.020
5	71.05	8.051	0.991	0.057
10	68.36	8.078	0.980	0.128
15	65.07	8.137	0.970	0.189
20	62.41	8.154	0.962	0.246
25	59.66	8.261	0.953	0.305
30	55.62	8.378	0.940	0.368
Dielectric parameters of the MetHb solution in PBS at 25 °C				
2.5	70.77	8.215	0.986	1.669
5	68.35	8.136	0.972	1.667
10	65.41	8.139	0.969	1.646
15	61.93	8.155	0.955	1.577
20	59.23	8.231	0.945	1.468
25	57.35	8.321	0.932	1.434
30	55.59	8.522	0.925	1.291

APPENDIX B: CALCULATION OF $\langle M^2 \rangle$ FOR MetHb SOLUTION IN DDW

The relationship between the values of Froehlich's B function for the MetHb aqueous solution and the number of hydrated water molecules was established using the model for the average square of the fluctuation dipole moment system. To average the squared random realization of the dipole momentum, it is necessary to determine the number of free water molecules in the sample—N_{free}—and the moment $\boldsymbol{M_{Hb}}$ in (6). We defined N_{free} as the number of bulk water molecules minus the number of water molecules associated with MetHb molecules in the volume V. In turn, the number of water molecules bounded by a single MetHb molecule can be determined using the number of positive, N_p, and negative, N_n, charges in the structure of the MetHb molecule.[34,35] It has recently been shown[36] that in the vicinity of the macromolecule in solution, the first two hydrated layers are well-organized and structured, and the second two layers have quite fast exchange with the bulk water. The simulations and theoretical calculations estimate this range as ~6 Å. All the detailed analyses of this statement are discussed elsewhere.[34] Thus, as a random implementation of $\boldsymbol{M_{Hb}}$ in the volume V, we will consider the following expression:

$$\boldsymbol{M}_{HB} = N_{Hb}\left(\sum_{i=1}^{N_p}\sum_{k=1}^{HN^{+}_{w6A}}\mu_{ik} + \sum_{i=1}^{N_n}\sum_{k=1}^{HN^{-}_{w6A}}\mu_{ik}\right), \tag{B1}$$

$$HN^{+}_{w6A} = \frac{N^{+}_{wb}}{N_p}, HN^{-}_{w6A} = \frac{N^{-}_{wb}}{N_n}, \tag{B2}$$

where N^{+}_{wb} and N^{-}_{wb} are the total numbers of water molecules hydrated by positive and negative charges of the single MetHb macromolecule.[34] Taking into account (B1) and (B2), the total random dipole moment of MetHb in DDW can be presented as follows:

$$\boldsymbol{M_{DDW}} = \sum_{i=1}^{N_{free}}\boldsymbol{\mu}_i + N_{Hb}\left(\sum_{i=1}^{N_p}\sum_{k=1}^{HN^{+}_{w6A}}\mu_{ik} + \sum_{i=1}^{N_n}\sum_{k=1}^{HN^{-}_{w6A}}\mu_{ik}\right). \tag{B3}$$

The mean square averaging of this value can be presented as follows:[34]

$$\left\langle M^2_{DDW}\right\rangle = N_{free}\mu^2 g_w + N_b^{(DDW)}\mu^2\left[1 - 4\left(\frac{N_p}{N_p + N_n}\right)\right], \tag{B4}$$

where $N_b^{(DDW)}$ is the number of water molecules hydrated by the MetHb macromolecules, and the number of free water molecules N_{free} is the difference between the number of bulk water molecules N_0 and $N_b^{(DDW)}$ in the volume V,

$$N_{free} = N_0 - N_b^{(DDW)}. \tag{B5}$$

Taking into account the relationship (B5), expression (B4) can finally be rewritten as

$$\left\langle M^2_{DDW}\right\rangle = N_0\mu^2 g_w\left\{1 - \frac{N_b^{(DDW)}}{N_0}\left[1 + 4\left(\frac{N_p}{N_p + N_n}\right)\right]\right\}. \tag{B6}$$

Dividing $\left\langle M^2_{DDW}\right\rangle$ by the sample volume V, we can obtain the mean square of the total fluctuating dipole moment of the unit volume as follows:

$$\frac{\left\langle M^2_{DDW}\right\rangle}{V} = n_0\mu^2 g_w\left\{1 - \frac{n_b^{(DDW)}}{n_0}\left[1 + 4\left(\frac{n_p}{n_p + m_n}\right)\right]\right\}, \tag{B7}$$

where

$$n_0 = \frac{N_0}{V}, \quad n_b^{(DDW)} = \frac{N_b^{(DDW)}}{V}, \quad n_p = \frac{N_{Hb}N_p}{V} \text{ and } n_n = \frac{N_{Hb}N_n}{V}. \tag{B8}$$

APPENDIX C: CALCULATION OF $\langle M^2 \rangle$ FOR MetHb SOLUTION IN PBS

For the MetHb solution in PBS, it is necessary to take into account the number of water molecules hydrated by ions of PBS using the additional term $\Delta \boldsymbol{M}$ in the random dipole moment of the aqueous solution (6),

$$\boldsymbol{M}_{PBS} = \boldsymbol{M}_{DDW} + \Delta \boldsymbol{M}, \tag{C1}$$

where

$$\Delta \boldsymbol{M} = \sum_{i=1}^{N_{jp}} \sum_{k=1}^{N_{jw}^{+}} \boldsymbol{\mu}_{ik} + \sum_{i=1}^{N_{jn}} \sum_{k=1}^{N_{jw}^{-}} \boldsymbol{\mu}_{ik}. \tag{C2}$$

Here, N_{jp} and N_{jn} are the numbers of positive and negative ions of PBS in the volume V of solution, and N_{jw}^{+} and N_{jw}^{-} are its average hydration numbers in the shells of all positive and all negative PBS ions, respectively.[34]

The average squared moment can be presented as follows:

$$\left\langle \boldsymbol{M}_{PBS}^2 \right\rangle = \left\langle \boldsymbol{M}_{DDW}^2 \right\rangle + \left\langle \boldsymbol{DM}^2 \right\rangle, \tag{C3}$$

where

$$\left\langle \boldsymbol{DM}^2 \right\rangle = 2\langle \boldsymbol{M}_{DDW} \cdot \Delta \boldsymbol{M} \rangle + \left\langle (\Delta \boldsymbol{M})^2 \right\rangle. \tag{C4}$$

Based on the assumptions described above and taking into account (C4), the mean square of the total fluctuating dipole moment of MetHb in PBS solution can be presented as follows:

$$\begin{aligned} \left\langle (\boldsymbol{M}_{PBS})^2 \right\rangle = N_0 \mu^2 g_w \Bigg\{ 1 - \frac{N_b^{(PBS)}}{N_0} \Bigg[1 + \frac{4}{g_w} \left(\frac{N_p}{N_p + N_n} \right)^2 \\ + \frac{4}{g_w} \left(\frac{N}{N_{Hb}\Delta N_n + N_{jp}} \right)^2 \Bigg] \\ - \frac{N_{jwb}}{N_0} \left[1 - \frac{1}{g_w} + \frac{4}{g_w} \left(\frac{N_{jn}}{N + N_{jp}} \right)^2 \right] \Bigg\}. \end{aligned} \tag{C5}$$

Here, $N_b^{(PBS)}$ is the number of water molecules hydrated by the MetHb macromolecules, and N_{jwb} is the total number of water molecules bounded by PBS ions,

$$N_{jwb} = N_{jp} \cdot N_{jw}^{+} + N_{jn} \cdot N_{jw}^{-}. \tag{C6}$$

The ratio $\frac{\langle (\boldsymbol{M}_{PBS})^2 \rangle}{V}$ is then

$$\begin{aligned} \frac{\left\langle (\boldsymbol{M}_{PBS})^2 \right\rangle}{V} = n_0 \mu^2 g_w \Bigg\{ 1 - \frac{n_b^{(PBS)}}{n_0} \Bigg[1 + \frac{4}{g_w} \left(\frac{n_p}{n_p + n_n} \right)^2 \\ + \frac{4}{g_w} \left(\frac{n_{jp}}{n_{Hb}\Delta N_n + n_{jp}} \right)^2 \Bigg] \\ - \frac{n_{jwb}}{N_0} \left[1 - \frac{1}{g_w} + \frac{4}{g_w} \left(\frac{n_{jn}}{n_{jn} + n_{jp}} \right)^2 \right] \Bigg\}, \end{aligned} \tag{C7}$$

where

$$n_{jp} = \frac{N_{jp}}{V}, \quad n_{jn} = \frac{N_{jn}}{V}, \quad n_{jwb} = \frac{N_{jwb}}{V}. \tag{C8}$$

DATA AVAILABILITY

The data that support the findings of this study are available within the article.

REFERENCES

[1] M. Henry, Cell. Mol. Biol. **51**, 677–702 (2005); available at https://pubmed.ncbi.nlm.nih.gov/16359619/.
[2] J. Caldecott, *Water: Life in Every Drop* (Virgin Digital, 2008).
[3] E. Levy *et al.*, J. Chem. Phys. **136**, 114502 (2012).
[4] E. Levy *et al.*, J. Chem. Phys. **136**, 114503 (2012).
[5] A. Puzenko *et al.*, J. Chem. Phys. **137**, 194502 (2012).
[6] E. Levy *et al.*, J. Chem. Phys. **140**, 135104 (2014).
[7] M. Chaplin, Nat. Rev. Mol. Cell Biol. **7**, 861 (2006).
[8] K. L. Ngai *et al.*, Philos. Mag. **91**, 1809 (2011).
[9] S. Bone and R. Pethig, J. Mol. Biol. **157**, 571 (1982).
[10] D. R. Martin and D. V. Matyushov, J. Phys. Chem. Lett. **6**, 407 (2015).
[11] S. K. Pal, J. Peon, and A. H. Zewail, Proc. Natl. Acad. Sci. U. S. A. **99**, 1763 (2002).
[12] J. A. Rupley, E. Gratton, and G. Careri, Trends Biochem. Sci. **8**, 18 (1983).
[13] L. Schilling, S. Palese, and D. Miller, "Laser spectroscopy of biomolecules," Proc. SPIE **1921**, 249–253 (1992).
[14] U. Kaatze, J. Chem. Phys. Eng. Data **34**, 371 (1989).
[15] W. J. Ellison, K. Lamkaouchi, and J.-M. Moreau, J. Mol. Liq. **68**, 171 (1996).
[16] A. Puzenko, P. Ben Ishai, and Y. Feldman, Phys. Rev. Lett. **105**, 037601 (2010).
[17] Y. Feldman *et al.*, Colloids Polym. **29**, 1923 (2014).
[18] E. H. Grant *et al.*, Bioelectromagnetics **7**, 151 (1986).
[19] E. H. Grant, R. J. Sheppard, and G. P. South, *Dielectric Behaviour of Biological Molecules in Solution* (Oxford University Press, Oxford, 1978).
[20] M. Wolf *et al.*, Biochim. Biophys. Acta, Proteins Proteomics **1824**, 723 (2012).
[21] C. Cametti, S. Marchetti, and G. Onori, J. Phys. Chem. B **117**, 104–110 (2013).
[22] S. Khodadadi, J. E. Curtis, and A. P. Sokolov, J. Phys. Chem. B **115**, 6222 (2011).
[23] K. S. Cole and R. H. Cole, J. Chem. Phys. **9**, 341 (1941).
[24] P. Debye, *Polar Molecules* (Dover, New York, 1929).
[25] I. Popov *et al.*, Phys. Chem. Chem. Phys. **18**, 13941 (2016).
[26] M. A. Vasilyeva *et al.*, Clays Clay Miner. **62**, 62 (2014).
[27] A. Caduff, P. Ben Ishai, and Y. Feldman, Biophys. Rev. **11**, 1017 (2019).
[28] D. Whitford, *Proteins: Structure and Function* (John Wiley & Sons, 2013).
[29] M. Chevion, Y. A. Ilan, A. Samuni, T. Navok, and G. Czapski, J. Biological Chemistry **254**(14), 6370-4 (1979); available at https://pubmed.ncbi.nlm.nih.gov/36393.
[30] K. Talley and E. Alexov, Proteins: Struct., Funct., Bioinf. **78**, 2699 (2010).
[31] N. Axelrod *et al.*, Meas. Sci. Technol. **15**, 755 (2004).
[32] R. Buchner, G. T. Hefter, and P. M. May, J. Chem. Phys. A **103**, 1 (1999).
[33] H. Fröhlich, *Theory of Dielectrics: Dielectric Constant and Dielectric Loss*, Monographs on the Physics and Chemistry of Materials, 2nd ed. (Clarendon Press, Oxford, 1958).
[34] L. Latypova *et al.*, "Oxygenation state of hemoglobin defines dynamics of water molecules in its vicinity," Phys. Chem. Chem. Phys. (unpublished) (2020).
[35] B. Qiao *et al.*, Proc. Natl. Acad. Sci. U. S. A. **116**, 19274 (2019).
[36] J. N. Dahanayake and K. R. Mitchell-Koch, Front. Mol. Biosci. **5**, 650 (2018).